

Consideration of Thin Film Ionization Vacuum Pressure Sensor

Marko Bošković, Danijela Randjelović, *Member, IEEE*, Milena Rašljčić, Katarina Cvetanović-Zobenica, Žarko Lazić, Milče M. Smiljanić, and Milija Sarajlić, *Member, IEEE*

Abstract— A novel concept of vacuum pressure sensor based on thin film technology is presented. The sensor is designed as a 1 μm thick aluminium film patterned as a structure of wedges facing each other along a sharp tip. The distance between the wedge tips is 3 μm . This structure is obtained by laser writing in vector mode. Parts of the sensor structure are fabricated and measured. Analytical consideration of the proposed structure is given together with the concept of the experimental set up for testing of the sensor.

Index Terms—Pressure sensor; DC discharge; Electrical conductivity of gases.

I. INTRODUCTION

Vacuum technology is very important in many scientific disciplines and industrial processes [1]. Measurement of the vacuum pressure depends on the range of vacuum, namely rough vacuum, medium vacuum, high or ultra-high vacuum (UHV). For measurements of rough vacuum, from atmospheric pressure down to 0.1 Pa, gauges like Pirani or mechanical manometers are used [2, 3, 4]. For high vacuum, or pressure lower than 0.1 Pa ionization gauges are used [5].

In this work, an ionization sensor of vacuum is designed, modelled by analytical formulas, and part of it is fabricated. Fabrication in the proposed technology of direct laser writing is feasible but it takes relatively long time for the machine to finish one production cycle.

Aim of this work is to examine whether it is possible to determine gas pressure by measuring the conductivity of gases with a microdevice. In the following, proposed sensor design and discussion of the proposed design pattern are given. Characteristics of fabricated sensor part are examined by Atomic Force Microscopy measurements. Afterwards, some theoretical background of electrical conductivity in gases is considered and calculations for proposed structure are performed. Last part of paper gives proposal for measurement set-up and schematic for calibration of the sensor.

Marko Bošković is with the ICTM-CMT, University of Belgrade, Studentski trg 16, 11000 Belgrade, Serbia (e-mail: boskovic@nanosys.ihtm.bg.ac.rs).

Danijela Randjelović is with the ICTM-CMT, University of Belgrade, Studentski trg 16, 11000 Belgrade, Serbia (e-mail: danijela@nanosys.ihtm.bg.ac.rs).

Milena Rašljčić is with the ICTM-CMT, University of Belgrade, Studentski trg 16, 11000 Belgrade, Serbia (e-mail: milena@nanosys.ihtm.bg.ac.rs).

Katarina Cvetanović-Zobenica is with the ICTM-CMT, University of Belgrade, Studentski trg 16, 11000 Belgrade, Serbia (e-mail: katarina@nanosys.ihtm.bg.ac.rs).

Žarko Lazić is with the ICTM-CMT, University of Belgrade, Studentski trg 16, 11000 Belgrade, Serbia (e-mail: zlazic@nanosys.ihtm.bg.ac.rs).

Milče M. Smiljanić is with the ICTM-CMT, University of Belgrade, Studentski trg 16, 11000 Belgrade, Serbia (e-mail: smilce@nanosys.ihtm.bg.ac.rs).

Milija Sarajlić is with the ICTM-CMT, University of Belgrade, Studentski trg 16, 11000 Belgrade, Serbia (e-mail: milijas@nanosys.ihtm.bg.ac.rs).

II. SENSOR DESIGN AND FABRICATION

The sensor is designed in four bunches, each with two pads. Each bunch consists of four stripes on one pad and five on another, with wedges which make a fringe pattern between them, Fig. 1. Each stripe is patterned on both sides with a series of wedges which are facing the wedges of the opposite stripe along the sharp tip. Enlarged detail of fringes (red rectangle in Fig. 1) is given in Fig. 2. The shortest distance between the tips is 3 μm .

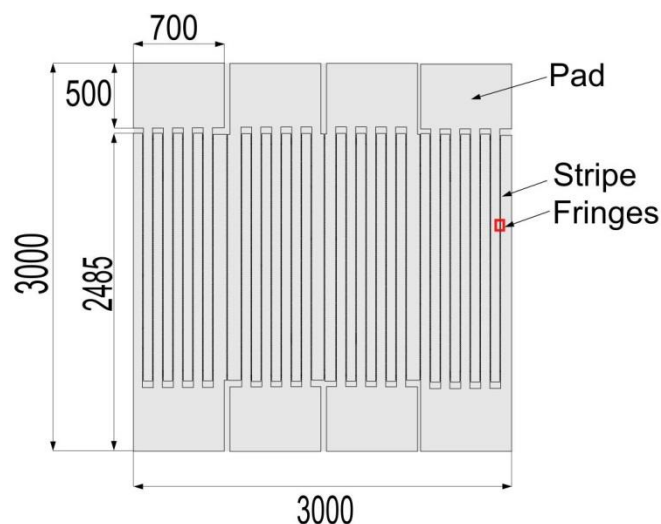


Fig. 1. Proposed design of the vacuum pressure sensor. Red rectangle is shown in Fig. 2. All units are in micrometers.

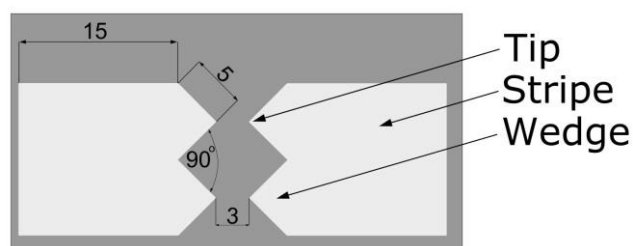


Fig. 2. Enlarged detail of the proposed design (red rectangle in Fig. 2). Units are in micrometers.

The technology needed for the fabrication of this type of the designed structures was already developed at ICTM-CMT [6]. With this technology, it was possible to fabricate the lines with the period of 6 μm and clearance between 2 μm and 3 μm using Laser Writer (LW405, MicroTech, Italy) in vector mode. Vector mode enables a machine to draw continuous lines and the width of the line is defined by the time of photoresist exposure and subsequent development.

A part of the proposed pattern for the vacuum pressure sensor is shown in Fig. 3.

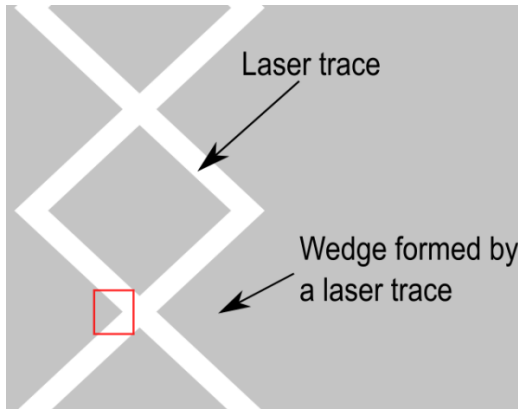


Fig. 3. A detail of proposed pattern and marked area where AFM scan was performed (red square).

The white line in Fig. 3 represents areas of wafer which will be exposed to laser radiation. After photolithography, we get structure similar to the structure shown in Fig. 2. If lines are 2 μm wide and are crossing each other on 90 degrees angle, calculated distance between wedge tips (electrodes) is 2.83 μm . Pattern was drawn using CleWin software [7].

The sensor was fabricated in a planar technology used for microelectronic devices. On a 3 inch wafer, 380 μm thick, $\langle 100 \rangle$ orientation, 3-5 Ωcm resistivity, n-type, one side polished, SiO_2 layer was grown by thermal oxidation at 1100 $^\circ\text{C}$ for 105 minutes. After thermal oxidation aluminium with 1% of silicon (Al 1% Si) was sputtered by DC Magnetron Sputtering. The wafer was then coated with photoresist AZ 1505 (MicroChemicals, Germany), 0.5 μm thick by spin coating. The wafer prepared in this way was then exposed to laser radiation (405 nm wavelength) using direct laser writer (LW405, MicroTech, Italy, 405 nm wavelength) in vector mode. After exposure, photoresist was developed using MIF 726 (MicroChemicals, Germany) developer for 25 seconds. Afterwards, photoresist was baked at 115 $^\circ\text{C}$ for 50 seconds. The next procedure was removal of aluminium from the exposed areas. This was done with a solution made of acetic acid, phosphoric acid and nitric acid. After this, the remained photoresist was removed with acetone.

In order to explore characteristics of lines fabricated in vector mode, Atomic Force Microscopy (AFM) measurement was performed. The structure on which AFM measurement was performed is marked as red square in Fig. 3. A 3D AFM scanning along the transition area between sputtered Al 1% Si and SiO_2 is shown in Fig. 4. Fig. 5 gives 2D image of the same structure. The profile of the transition (red line in Fig. 5) is shown in Fig. 6.

Thickness of sputtered Al 1% Si is estimated to be around 0.7 μm from Fig. 6 and surface roughness is around 73 nm, Fig 6.

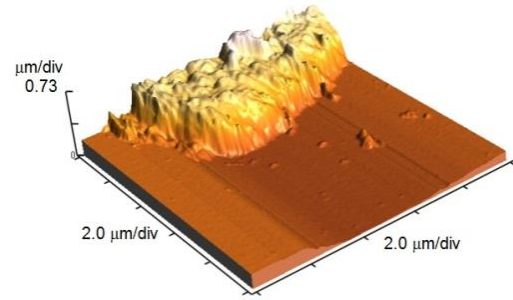


Fig. 4. 3D AFM picture of the obtained structure

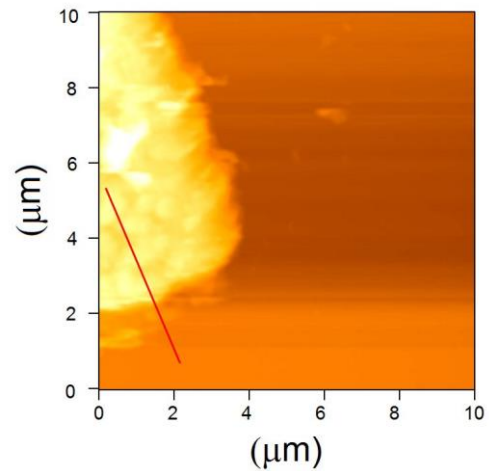


Fig. 5. 2D AFM image with the profile line marked red.

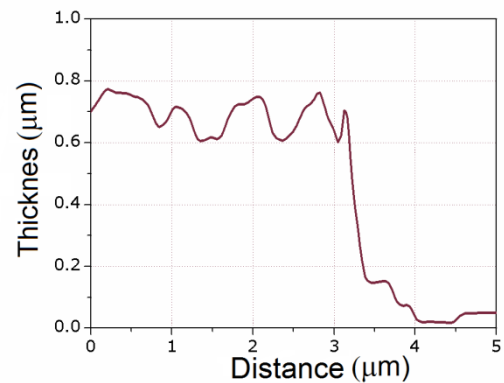


Fig. 6. profile of the characteristic line.

III. ANALYTICAL MODEL OF SENSOR FUNCTIONALITY

Under normal conditions gas is behaving as an electrical insulator. Under certain conditions gas can conduct electricity [8]. The flow of the electrical current through gases is known as electrical discharge. There are three different types of electrical discharge – Townsend (dark) discharge, glow discharge and arc discharge. These types can be distinguished by current-voltage characteristics.

For the functionality of this sensor, the region of interest is Townsend discharge. In this region the applied voltage accelerates free ions and electrons so that certain number of them will reach the electrodes. The current is proportional to the applied voltage and gas acts as an Ohmic resistor. Further increasing of voltage allows all charged particles to reach the electrode and current enters the saturation. If the applied voltage is further increased, the current rapidly increases. This is a consequence of creating new ions in gas by collisions.

Ionization in this region is a consequence of three processes [9]:

-While moving toward anode electrons collide with gas particles and generate more electrons and ions;

-Positive ions moving toward the cathode collide with gas particles, ionize and also generate certain numbers of electrons and positive ions;

-Particles such as positive ions strike the cathode to emit secondary electrons.

Each of these processes is quantitatively characterized by three Townsend coefficients: α , β and γ respectively. Townsend coefficient α is the electron ionization coefficient for the volume of gas. If the number of accelerated electrons is n_{e0} and the gap between the electrodes is x than the number of produced electrons is [9]:

$$n_e = n_{e0} e^{\alpha x}, \quad (1)$$

and discharge current reaching the anode is [9]:

$$i_e = i_{e0} e^{\alpha x}. \quad (2)$$

Coefficient α depends on the mean free path of electrons, λ_e , and intensity of the electric field E . It can be calculated using equation [9]:

$$\alpha = \frac{1}{\lambda_e} \exp\left(-\frac{V_i}{E\lambda_e}\right), \quad (3)$$

where V_i is ionization energy of gas component.

Mean free path is the average distance travelled by particle between colliding. With approximation of the ideal gas state, mean free path can be calculated using equation [10]:

$$\lambda_e = \frac{kT}{\sqrt{2} p \pi d^2}, \quad (4)$$

where k is the Boltzmann constant, T is the gas temperature, p is the gas pressure and d is the effective diameter of the particle.

Equations (3) and (4) show that, for a specific gas α is a function of the gas pressure and the electric field intensity.

Coefficient β is a positive ion ionization coefficient. Required energy for positive ions to ionize neutral particles is thousands of electron volts. In a normal discharge process ions do not have this energy so a contribution of β is negligible [9].

Coefficient γ is the electrode surface ionization coefficient for positive ions. It shows how many electrons are emitted from the cathode when positive ion strikes it. If $n_0(e^{\alpha x} - 1)$ positive ions strike a cathode, the number of electrons

emitted from cathode will be $\gamma n_0(e^{\alpha x} - 1)$. Coefficient γ is a function of cathode material and kinetic energy of impact ions. Ions must have enough energy to overcome the electron binding energy of cathode material. Given that the kinetic energy of ions is determined by the intensity of the electric field and gas pressure, one can tell that coefficient γ is a function of gas pressure, intensity of the electric field and cathode material. Coefficient γ can be calculated using Baragiola empirical equation [11]:

$$\gamma = 0.032(0.78V - 2\phi), \quad (5)$$

or Hagstrum's semi empirical equation [11]:

$$\gamma = \frac{0.2(0.8V - 2\phi)}{\varepsilon_F}. \quad (6)$$

In both equations, V is the energy of incident ion, ϕ is the work function, and ε_F is the Fermi energy.

Total discharging current is [9]:

$$i_e = \frac{i_{e0} e^{\alpha x}}{1 - \gamma(e^{\alpha x} - 1)} \quad (7)$$

Total discharge current is a function of Townsend coefficients, thus, it is a function of pressure and intensity of electric field.

Total discharge current as a function of pressure was calculated for various values of the electric field intensity and for various gases. Total discharge current was calculated using (7). The work function of aluminium is 4.25 eV [12] so electrode surface ionization coefficient (γ) contribution is negligible for the considered voltages. Electron ionization coefficient was calculated using (3), and mean free path was calculated using (4).

Total discharge current versus pressure for argon and molecules of nitrogen and oxygen is shown in Fig. 7. Pressure range is between $1 \cdot 10^5$ Pa and $7 \cdot 10^5$ Pa. Ionization energies are 15.763 eV for argon [13], 12.0697 eV for oxygen [14] and 15.581 eV for nitrogen [15]. Kinetic diameters are 340 pm for argon [16], 346 pm for oxygen [17], and 364 pm for nitrogen [17].

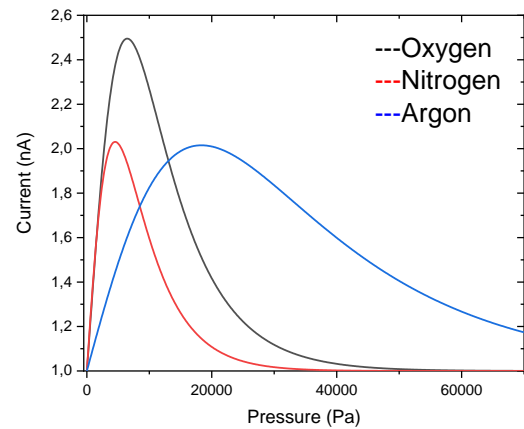


Fig. 7. Current versus pressure for O_2 , N_2 and Ar for intensity of electric field of $1 \cdot 10^7$ V/m.

Total discharge current for various intensities of the electric field is shown in Fig. 8.

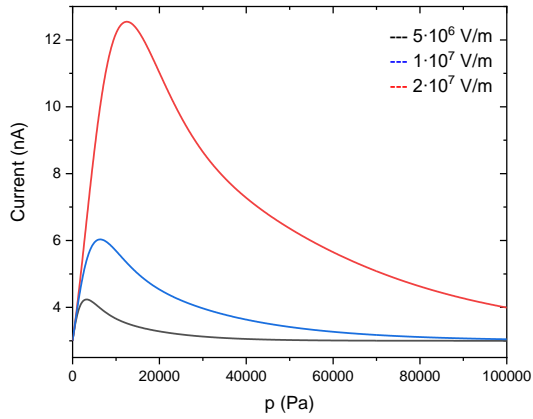


Fig. 8. Total discharge current versus pressure for different intensity of the electric field for Ar, O₂, and N₂.

Influence of the intensity of the electric field (i.e. applied voltage) can be understood from the plot of total current vs. pressure for various intensities of electric field, Fig. 8.

Fig. 8. shows that current has maximum values on 2300 Pa, 4500 Pa and 9000 Pa for intensity of the electric field of $5 \cdot 10^6$ V/m, $1 \cdot 10^7$ V/m, and $2 \cdot 10^7$ V/m, respectively.

Applying different voltage on sensor pads can provide required pressure range.

Current in Fig. 7, and Fig. 8 is calculated for one pair of wedges (Fig. 2). In a single bunch there are 2110 pairs of wedges and in whole sensor, there are 9240 pairs of wedges, so current has to be multiplied by these factors.

IV. PROPOSAL OF THE EXPERIMENT

Fig. 9 shows simplified scheme of measurement set-up.

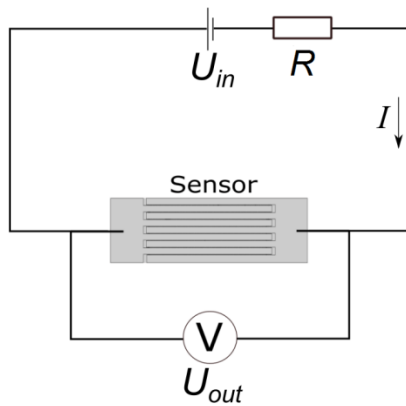


Fig. 9. Simplified scheme of the measurement principle.

Principle of operation can be understood from Fig. 9. Voltage is applied on pads of one bunch. If, for given voltage, gas pressure is above pressure upper limit for which gas between wedges is conductive there will be no current flow through a circuit (resistance of gas between opposite wedges is infinite) and output voltage will be the same as the input voltage, $U_{out} = U_{in}$. If the applied voltage is increased, or if the pressure is reduced, gas between wedges will become conductive and there will be current flow through the circuit. The output voltage will be lower and could be calculated using the equation:

$$U_{out} = U_{in} - IR, \quad (8)$$

where I is the current through the circuit and R is the resistance, Fig. 9. Current in a circuit is a total discharge current (7). Further reduction of the pressure will alter Townsend coefficients and change discharge current and, according to (8), the change in current will give different output voltage.

In the proposed design sensor consists out of four bunches identical with one on Fig. 9 (labelled as sensor). These bunches can be connected in parallel if the current in one bunch is not large enough to be detected.

Schematic for calibration of the sensor is shown in Fig. 10.

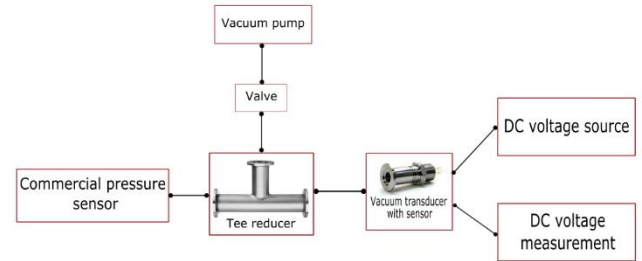


Fig. 10. Block scheme of sensor calibration experiment.

Calibration of the sensor could be done by a recording of the sensor voltage drop as a function of the pressure for a given intensity of the electric field. The pressure should be slowly reduced using a vacuum pump and control valve. The pressure value can be controlled by the commercial pressure sensor. Voltage drop should be measured for different pressure values using appropriate electronics. As a result, the voltage vs. pressure curve could be obtained which may serve as a calibration curve for the sensor.

V. CONCLUSION

Design and analytical model for planar pressure sensor have been presented. It was shown that it is feasible to fabricate the desired structure using direct laser writing. Calculations based on the presented analytical model have been done for different gases and for various intensities of the electric field. Calculations showed that measurable current-dependence of pressure can be accomplished for a wide range of pressure by applying different voltages. The proposed sensor design seems to be a competitive microscopic device for measuring pressure in a wide vacuum range.

ACKNOWLEDGMENT

This work was supported by the Serbian Ministry of Education, Science and Technological Development under the project TR32008.

REFERENCES

- [1] J. H. Leck, *Total and Partial Pressure Measurement in Vacuum Systems*, 1st edition, London, England: Springer Science & Business Media, 2012.
- [2] D. Randjelović, A. Petropoulos, G. Kaltsas, M. Stojanović, Ž. Lazić, Z. Djurić, M. Matic, "Multipurpose MEMS Thermal Sensor Based on

- Thermopiles“, *Sensors and Actuators A, Sensors and Actuators A: Physical*, Vol. 141, Issue 2, pp. 404-413, February, 2008.
- [3] D. V. Randjelović, M. P. Frantlović, B. L. Miljković, B. M. Popović, Z. S. Jakšić, “Intelligent Thermal Vacuum Sensors Based on Multipurpose Thermopile MEMS Chips“, *Vacuum*, Vol. 101, pp. 118-124, March, 2014.
- [4] D. Randjelović, V. Jovanov, Ž. Lazić, Z. Djurić, M. Matić, “Vacuum MEMS Sensor Based on Thermopiles – Simple Model and Experimental Results“, Proc. 26th International Conference on Microelectronics MIEL 2008, Niš, Serbia, vol. 2, pp. 367-370, 11.-14.5.2008.
- [5] G.J. Schulz, A.V. Phelps, “Ionization Gauges for Measuring Pressures up to the Millimeter Range,” *Review of Scientific Instruments*, vol. 28, no. 12, 1051-1054, December, 1957.
- [6] M. Sarajlić, M. M. Smiljanić, Ž. Lazić, K. Cvetanović-Zobenica, D. Randjelović and D. Vasiljević-Radović, “Direct Laser Writing of micro-structures in vector mode for chemical sensors” Proc. 5th International conference IcETRAN, Palic, Serbia, pp. 949-952, 11.-14.06.2018.
- [7] Clewin Software <https://wieweb.com/site/>, Accessed 15.02.2019.
- [8] J.J. Thomson, *Conduction of Electricity through Gases*, 2nd edition, London, England: Cambridge: At the university press, 1906.
- [9] D. Xiao, *Gas discharge and gas insulation*, 1st edition, Shanghai, China: Shanghai Jiao Tong University Press, Springer, 2016.
- [10] R. D. Levine, *Molecular Reaction Dynamics*, 1st edition, New York, United States of America: Cambridge University press, 2005.
- [11] Y. Yamauchi, R. Shimizu, “Secondary Electron Emission from Aluminium by Argon and Oxygen Ion Bombardment below 3 keV,” *Japanese Journal of Applied Physics*, vol. 22, no. 4, pp. 227-229, April, 1983.
- [12] E. William, J. Mitchell and J. W. Mitchell, “The work function of copper, silver and aluminium” *The Royal Society publishing*, vol. 120, pp. 70-84, December, 1951.
- [13] K. M. Weitzel, J. Mahnert, M. Penno, “ZEKE-PEPICO investigations of dissociation energies in ionic reactions,” *Chemical physics letters*, vol. 224, pp. 371-380, July, 1994.
- [14] R. G. Tonkyn, J. W. Winniczek, M. G. White, “Rotationally resolved photoionization of O₂ near threshold”, *Chemical Physics Letters*, vol. 164, pp. 137-142, December, 1989.
- [15] T. Trickl, E. F. Cromwell, Y. T. Lee, A. H. Kung, “State-selective ionization of nitrogen in the X₂=0 and v=1 states by two-color (1+1) photon excitation near threshold”, *Journal of Chemical Physics*, vol. 91, pp. 6006-6012, November, 1989.
- [16] D. W. Breck, *Zeolite Molecular Sieves: Structure, Chemistry and Use*, 1st edition, New York: Wiley, 1973.
- [17] A. F. Ismail, K.C. Khulbe, T. Matsuura, *Gas separation membranes*, 1st edition, Basel, Switzerland: Springer International Publishing Switzerland, 2015.